

ARL-FLIGHT-MECH-R-191

AR-007-083

**AD-A259 624**



**DEPARTMENT OF DEFENCE**  
**DEFENCE SCIENCE AND TECHNOLOGY ORGANISATION**  
**AERONAUTICAL RESEARCH LABORATORY**

**MELBOURNE, VICTORIA**

**Flight Mechanics Report 191**

**DTIC**  
**ELECTE**  
**JAN 27 1993**  
**S C D**

**VARIABLE CONTROL SYSTEM LIMITS ON BLACK HAWK**  
**AND SEAHAWK HELICOPTERS**

by

**J. BLACKWELL**  
**S. DUTTON**  
**R. TOFFOLETTO**  
**J.F. HARVEY**

Approved for public release.

© COMMONWEALTH OF AUSTRALIA 1992

OCTOBER 1992

**93-01461**



398

**98 1 26 077**

**This work is copyright. Apart from any fair dealing for the purpose of study, research, criticism or review, as permitted under the Copyright Act, no part may be reproduced by any process without written permission. Copyright is the responsibility of the Director Publishing and Marketing, AGPS. Enquiries should be directed to the Manager, AGPS Press, Australian Government Publishing Service, GPO Box 84, CANBERRA ACT 2601.**

**DEPARTMENT OF DEFENCE  
DEFENCE SCIENCE AND TECHNOLOGY ORGANISATION  
AERONAUTICAL RESEARCH LABORATORY**

Flight Mechanics Report 191

**VARIABLE CONTROL SYSTEM LIMITS ON BLACK HAWK  
AND SEAHAWK HELICOPTERS**

by

J. BLACKWELL  
S. DUTTON  
R. TOFFOLETTO  
J.F. HARVEY

**SUMMARY**

*Black Hawk and Seahawk helicopters have various fixed physical control limits situated throughout the control system. The range of each pilot control is variable and depends on which limit is reached first. This is a function of the pilot control inputs applied, together with any additional control inputs provided by the automatic flight control system. A procedure has been developed to monitor controls in the vicinity of each limit, and determine if any part of the control system approaches to within a prescribed amount of a limit. Warning lights in the cockpit inform the pilot if a limit is being approached. The procedure was used effectively during a First of Class Flight Trial involving a Black Hawk.*



DTIC QUALITY INSPECTED 5

© COMMONWEALTH OF AUSTRALIA 1992

**POSTAL ADDRESS:** Director, Aeronautical Research Laboratory  
506 Lorimer Street, Fishermens Bend 3207  
Victoria Australia

Accession For	
NTIS GRA&I	<input checked="" type="checkbox"/>
DTIC TAB	<input type="checkbox"/>
Unannounced	<input type="checkbox"/>
Justification	
By _____	
Distribution/	
Availability Codes	
Avail and/or	
Dist	Special
A-1	

## **CONTENTS**

### **NOTATION**

<b>1. INTRODUCTION</b>	<b>1</b>
<b>2. OVERVIEW OF BLACK HAWK AND SEAHAWK CONTROL SYSTEM</b>	<b>2</b>
<b>3. OUTLINE OF PROCEDURE TO DETERMINE CONTROL POSITIONS</b>	<b>5</b>
<b>4. RELATIONSHIP BETWEEN PRIMARY LATERAL AND LONGITUDINAL CONTROLS AND LIMITS</b>	<b>6</b>
<b>4.1 Roller Location</b>	<b>6</b>
<b>4.2 Limiter Geometry</b>	<b>7</b>
<b>4.3 Effect of Control Inputs on Roller Motion</b>	<b>9</b>
<b>4.4 Fraction of Possible Primary Control Movement</b>	<b>11</b>
<b>5. ALGORITHM TO OPERATE COCKPIT LIGHTS</b>	<b>13</b>
<b>5.1 General Description</b>	<b>13</b>
<b>5.2 Algorithm Details</b>	<b>16</b>
<b>6. PRELIMINARY RESULTS FROM FIRST OF CLASS FLIGHT TRIALS</b>	<b>20</b>
<b>6.1 Effect of Mechanical Control Mixing</b>	<b>20</b>
<b>6.2 Effect of AFCS Inputs</b>	<b>20</b>
<b>7. CONCLUDING REMARKS</b>	<b>24</b>
<b>ACKNOWLEDGMENTS</b>	<b>24</b>
<b>REFERENCES</b>	<b>24</b>
<b>APPENDICES</b>	
<b>DISTRIBUTION</b>	
<b>DOCUMENT CONTROL DATA</b>	

## NOTATION

a, b	x, z coordinates of circle centre in equation representing path of lateral or longitudinal roller centre as roller rolls along limiter
c	Fixed pivot separation distance on longitudinal potentiometer (Fig. 5)
C, E	Non-fixed pivots within mixing unit (Fig. 7)
D	Fixed pivot within mixing unit, location STA=292, WL=274 (Fig. 7)
D'	Experimentally deduced location of D prior to correction (Fig. 9)
E <sub>1</sub> , E <sub>2</sub> , E <sub>3</sub>	Experimentally deduced locations of pivot E for various collective settings (Fig. 9)
k	Fraction of allowable control movement (Fig. 10)
L	Distance between potentiometer pivots (Figs A1 and A2)
L <sub>1</sub> , L <sub>2</sub>	Variable lateral potentiometer lengths (Fig. 5)
L <sub>3</sub> , L <sub>4</sub>	Variable longitudinal potentiometer lengths (Fig. 5)
r	Radius of circle in equation representing path of lateral or longitudinal roller centre as roller rolls along limiter
R <sub>1</sub> , R <sub>2</sub>	Control linkage arm lengths (Fig. 7)
s	Length of arc between upper and lower primary limiters (Fig. 10)
STA	Station (-ve x direction) relative to standard datum (inches)
WL	Waterline (z direction) relative to standard datum (inches)
x	Distance in x direction (+ve x is forward) from D
x <sub>k</sub>	Value of x for roller located at fraction k of allowable control movement (Fig. 10)
x', x''	Value of x for roller on lower, upper limiter (Fig. 10)
z	Distance in z direction (+ve z is up) from D
z <sub>k</sub>	Value of z for roller located at fraction k of allowable control movement (Fig. 10)
z', z''	Value of z for roller on lower, upper limiter (Fig. 10)

## Acronyms

AFCS	Automatic Flight Control System
AMAFTU	Aircraft Maintenance and Flight Trials Unit
CG	Centre of Gravity
FOCFT	First of Class Flight Trial
FPS	Flight Path Stabilisation
LVDT	Linear Variable Differential Transformer
PBA	Pitch Bias Actuator
RAN	Royal Australian Navy
SAS	Stability Augmentation System
SHOL	Ship Helicopter Operating Limit

## 1. INTRODUCTION

The Aircraft Maintenance and Flight Trials Unit (AMAFU) of the Royal Australian Navy (RAN) conducts a First of Class Flight Trial (FOCFT) for each helicopter/ship combination in order to establish operational limits. An important requirement of FOCFTs is that the helicopter controls be instrumented and the pilot be given feedback as to whether any of the controls approach control limits. In 1990, AMAFTU conducted a preliminary trial with a RAN Seahawk helicopter operating from an FFG-7 frigate. More recently, AMAFTU conducted a FOCFT with a Black Hawk helicopter operating from the Heavy Landing Ship HMAS Tobruk (Ref. 1) and plans to conduct a FOCFT with a Seahawk operating from an FFG-7.

Black Hawk and Seahawk helicopters have a highly complex control system which includes mechanical mixing between controls to reduce pilot workload by coupling various controls to account for coupled responses to given control inputs, and an Automatic Flight Control System (AFCS) which enhances the stability and control characteristics of the helicopter. The AFCS provides additional control inputs which are a function of helicopter accelerations, attitudes, angular rates, and velocities. Details on the control system can be found in Ref. 2.

There are physical end stops in the control system which limit control movement. They are located between the pilot controls and the mixer unit (four secondary end stops), and between the mixer unit and the rotor blades (four primary end stops). The range of each pilot control is variable, depending on whether primary or secondary end stops are reached first, which is a function of the pilot control inputs being applied, together with additional control inputs from the AFCS.

It is desired to determine the location of controls relative to the various end stops in the control system, and in particular to determine when the aircraft controls have approached to within 10% of a control limit. It is quite feasible for controls to be more than 10% from secondary end stops yet within 10% of primary end stops or vice versa. To be confident that no end stops have been overlooked, instrumentation of controls relative to all eight end stops is required. The four secondary controls and primary tail and collective controls move linearly relative to fixed end stops. Instrumentation of these controls is relatively easy, as is determining remaining control movement. However, the lateral and longitudinal primary controls move in non-linear motion relative to curved limiters resulting in variable or "floating" end stops. Instrumentation of these controls, together with the development of an algorithm to determine control position relative to limits, is less straightforward. The preliminary Seahawk trial involved instrumentation of controls relative to the four secondary end stops and instrumentation of primary control rod positions relative to a fixed datum; however, no account of floating end stops was taken.

This document first presents an overview of the Black Hawk and Seahawk control systems, as well as the instrumentation of controls required for a FOCFT. It then covers in more detail the instrumentation of control positions relative to the primary lateral and longitudinal end stops. A procedure is then developed to determine the fraction of remaining primary control movement and display it to the pilot in real time. The preliminary Seahawk trial did not display the amount of available primary control remaining to the pilot except for tail rotor control. The work outlined in this document was carried out on a Black Hawk helicopter for a FOCFT with HMAS Tobruk in October 1991. A sample of preliminary results is given in Section 6. It is planned to use the procedures developed in this document during future FOCFTs with both Seahawk and Black Hawk helicopters.

## 2. OVERVIEW OF BLACK HAWK AND SEAHAWK CONTROL SYSTEM

The Black Hawk and Seahawk control system, comprising an AFCS and mechanical mixing unit together with various control end stops, is illustrated schematically in Fig. 1. Minor differences exist in the AFCS between the Black Hawk and Seahawk, e.g. in the "automatic depart" feature (Refs 3 and 4), but from the point of view of determining available control authority, the procedure developed in this document is applicable to both aircraft types.

The AFCS has both an outer loop and inner loop function. Outer loop operation provides control inputs which move the pilot controls. Inner loop operation provides additional control inputs between pilot controls and the mixer unit. The inner loop AFCS control inputs are important because the proximity of controls relative to primary limits can vary in spite of the pilot controls not being moved. Components of the inner loop AFCS are

- Stability Augmentation System (SAS) - enhances helicopter stability about the pitch, roll, and yaw axes (control authority of SAS is limited to  $\pm 10\%$  of total control travel in pitch, roll, and yaw)
- Pitch Bias Actuator (PBA) - improves static longitudinal stability

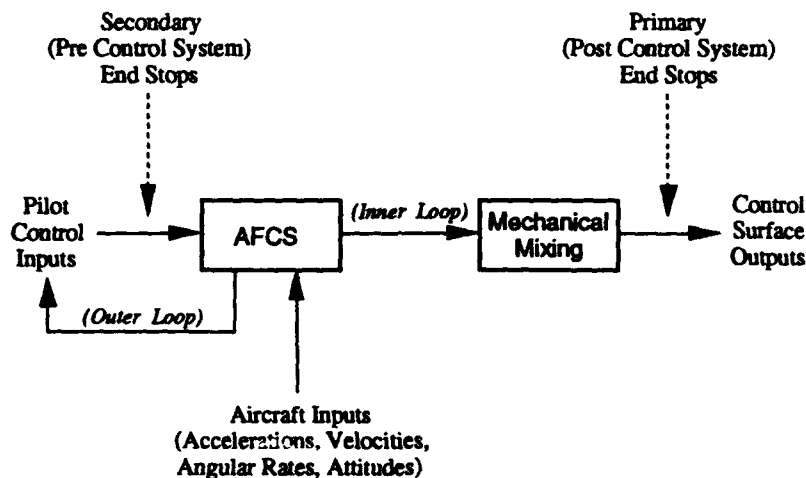
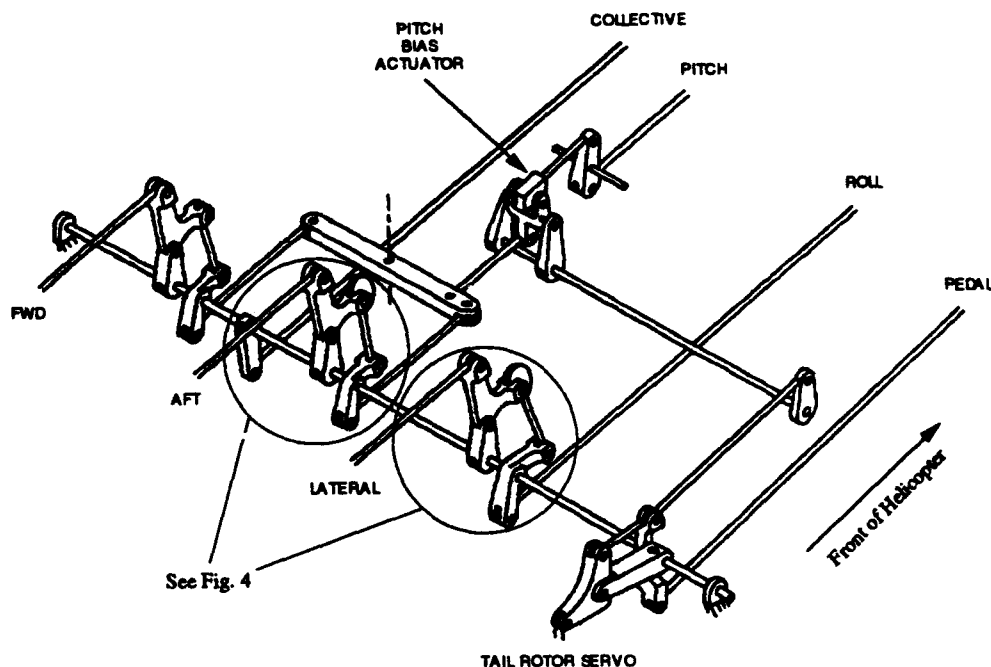


Fig. 1 Schematic Representation of Black Hawk and Seahawk Control System

Fig. 2 shows the mechanical mixing unit in schematic form. The PBA, which is part of the AFCS, is also shown. The mixing unit reduces pilot workload by mechanically coupling controls. For instance, there is a collective stick to tail rotor blade pitch coupling which automatically increases tail rotor thrust as collective is increased to allow for the increase in main rotor torque. Other mixing is collective stick to longitudinal cyclic, collective stick to lateral cyclic, and pedal to longitudinal cyclic. The pedal to longitudinal cyclic coupling is unique to helicopters with canted tail rotors, such as the Seahawk and Black Hawk, since a variation in tail rotor thrust produces not only a change in aircraft yaw but also a significant change in aircraft pitch. For more details on the AFCS or mixing unit, see Ref. 2.

There are eight physical end stops in the control system which limit control movement. Four secondary stops, located between the pilot controls and mixer unit, limit the pilot control movements directly. In addition, four primary stops, located between the mixer unit and the rotor blades, limit the motion of the control rods that operate main and tail blade pitch. The location of the primary and secondary limiters is summarised in Table 1.



**Fig. 2 Schematic Form of Black Hawk and Seahawk Mechanical Mixing Unit**

**TABLE 1**  
**Location of Primary and Secondary Limiters**

Limiter	Location of Limiter			
	Pedal/Tail Rotor	Collective	Longitudinal	Lateral
Secondary (Pre Control System)	Yaw Boost Assembly	Collective Stick	Cyclic Stick	Cyclic Stick
Primary (Post Control System)	Control Rod in Cabin Roof	Mixer Unit	Mixer Unit	Mixer Unit

If the AFCS is turned off, the relationship between primary and secondary end stops can be examined by constructing control limit envelopes or "nomograms". Fig. 3 shows schematic nomograms for a Black Hawk helicopter. The precise nomogram is specific to a given aircraft due to individual rigging of controls. In examining the first of the nomograms, it can be seen that at minimum collective the left pedal travel is limited by the secondary pedal stop but the right pedal travel is limited by the primary pedal stop. However, at full collective the left pedal is limited by the primary stop and the right pedal is limited by the secondary stop. With reference to the second nomogram, it should be noted that, depending on control rigging for a particular aircraft, the lateral right primary stop and lateral left secondary stop may not be reached even at zero collective and full right or left stick. At most, they are only reached for a small range of collective. The control position corresponding to 0 and 100% of each control movement is summarised in Table 2.



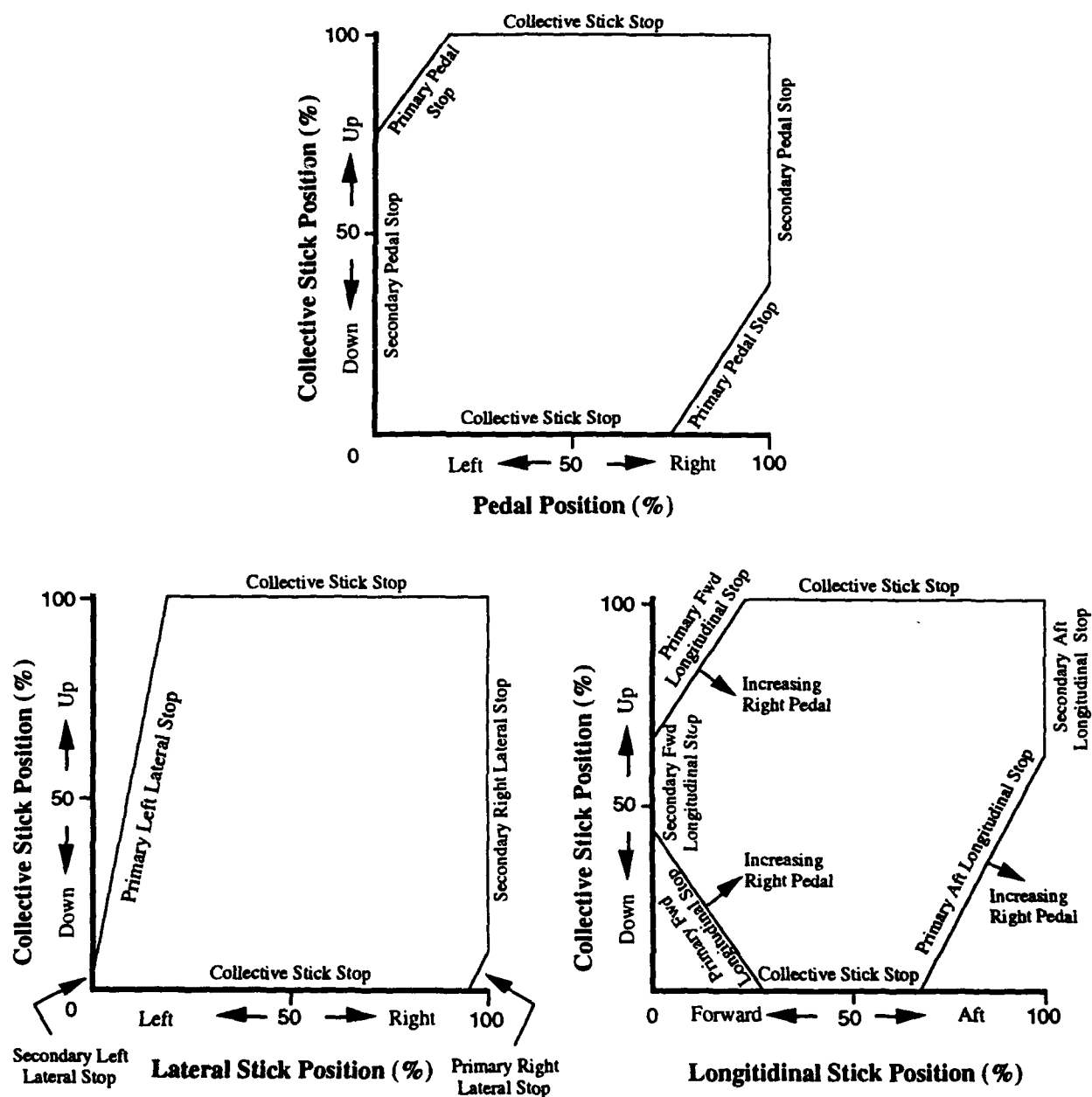


Fig. 3 Schematic Nomograms (Control Limit Envelopes)

TABLE 2  
Control Position Corresponding to Percentage of Control Movement

Percentage of Control Movement	Control Position			
	Pedal	Lateral	Longitudinal	Collective
0	Left	Left	Fwd	Down
100	Right	Right	Aft	Up

The nomograms do not take account of the additional control inputs supplied by the AFCS to the mixer unit. During a FOCFT, the RAN considers instances where less than 10% control

authority remains as outside the Ship Helicopter Operating Limit (SHOL) envelope. Since the additional AFCS control inputs may cause controls to be within 10% of their limits, even though nomograms show otherwise, the use of nomograms alone is not satisfactory. To determine whether one or more controls are outside the acceptable range during flight, when the AFCS would normally be operating, it was therefore decided to instrument controls in the vicinity of all eight end stops (four primary, four secondary). This provides a significant improvement over earlier control instrumentation in Seahawk trials where control position relative to the variable primary lateral and longitudinal end stops was not instrumented.

### 3. OUTLINE OF PROCEDURE TO DETERMINE CONTROL POSITIONS

Determining the position of the four pilot controls relative to the secondary end stops is performed indirectly by instrumenting control rods that are between the pilot controls and the mixer unit. The motion of the control rods is directly related to the pilot control positions. Linear Variable Differential Transformers (LVDTs), which are easy to calibrate, are used to record the control movement. The output is sent to four gauges in the cockpit to give the pilot continuous reading of percentage of control authority remaining, relative to the secondary stops only. This aspect of the instrumentation is unchanged from the earlier Seahawk trial.

Determining the position of two of the controls (tail and collective) relative to primary end stops is similarly straightforward. Tail and collective primary controls are instrumented using linear potentiometers. The amount of tail control authority available relative to primary end stops has been available on the earlier Seahawk trial. The primary collective control rod was instrumented in this earlier trial, but the location relative to primary end stops was not displayed to the pilot.

Instrumentation of the remaining two controls (lateral and longitudinal) relative to primary end stops is much less straightforward, as is the determining of the percentage of control authority remaining. Each of these controls is limited by a roller, which is connected to the control system by linkages, coming into contact with one of two curved surfaces, one above and one below. There is one roller to limit lateral control movement which is attached to a lateral control linkage, and one roller to limit longitudinal control movement which is attached to an aft control linkage (Fig. 2). A schematic showing a roller and associated control linkages is shown in Fig. 4. The control pivot D in the mixer unit, which remains fixed relative to the helicopter at station (STA) 292 and waterline (WL) 274, is used as a reference point in the procedure described below. Coordinates x and z refer to displacements (in inches) from D in the helicopter longitudinal (+ve forward) and vertical (+ve up) axes respectively.

Since the rollers are located within the mixer unit, there is limited space available to introduce transducers to record the roller position. In addition, the path taken by each roller as a function of pilot control inputs is far from linear. The position of the longitudinal roller is a function of collective, pedal, and longitudinal inputs, while the position of the lateral roller is a function of collective and lateral inputs (these inputs include those supplied by the AFCS). The point where each roller strikes its curved limiters, thus restricting roller motion, depends on the combination of control inputs. This results in infinitely variable or "floating" end stops for the primary cyclic controls. The transducer fit required to determine roller location is discussed in Section 4.1.

After instrumentation of the controls relative to primary end stops, the output is analysed in real time by a computer algorithm which determines whether any control is within 15% of a primary limit (an amber light is turned on in the cockpit - one for each control) or within 10% of a primary limit (a single red light is turned on). In this way the pilot receives instant feedback as to the location of the controls relative to primary end stops. By monitoring gauges and lights, it is possible to determine if any part of the control system comes within 15 or 10% of a limit. In addition, the data representing control position relative to the four primary and the four secondary

end stops are recorded by a system called VADAR (Versatile Airborne Data Acquisition and Replay) developed at ARL (Ref. 5) for post-trial analysis.

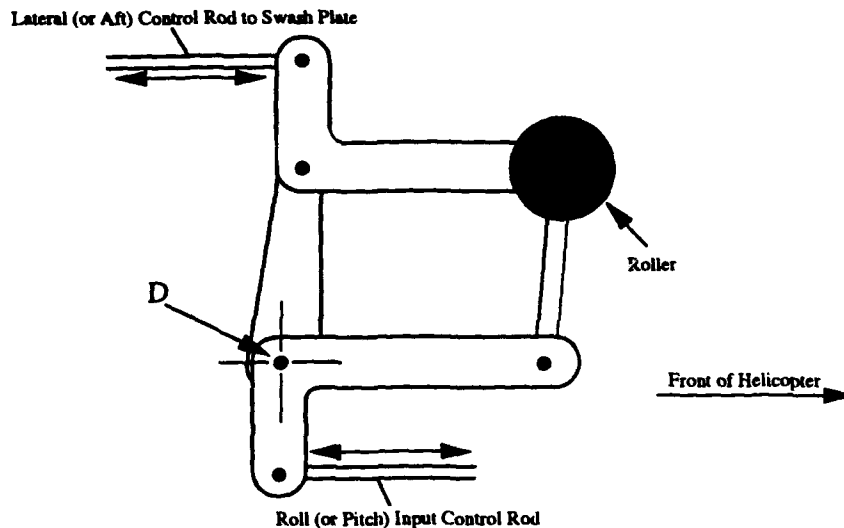


**Fig. 4 Schematic Showing Lateral (or Longitudinal) Roller and Attached Linkages in Mixer Unit (D is Fixed Control Pivot Reference Point at STA=292, WL=274)**

#### **4. RELATIONSHIP BETWEEN PRIMARY LATERAL AND LONGITUDINAL CONTROLS AND LIMITS**

Initially, a procedure for determining the location of the lateral and longitudinal rollers is deduced (Section 4.1), and the geometry of the primary limiters determined (Section 4.2). The motion of each roller for pure cyclic inputs is ascertained (Section 4.3) and used to determine the fraction of available control movement for a given roller location (Section 4.4). The location of the rollers is recorded on VADAR for post trial analysis, and is also analysed in real time to operate cockpit lights when appropriate (Section 5).

##### **4.1 Roller Location**

The location of each roller was determined from the lengths of four linear potentiometers, with two mounted per roller (Fig. 5). Due to the limited space available, the location of the potentiometers was not ideal. In addition, modification of the cowling on top of the mixer unit was required to make room for the longitudinal potentiometers. The pivot locations relative to D are given in Table 3. This reference point was selected because it corresponds to a control pivot in the mixer unit which remains fixed at all times relative to the helicopter. Signals from the potentiometers were converted from raw data to length (in inches) by the data acquisition system. The location of the roller centre,  $(x,z)$ , can then be determined from the potentiometer lengths,  $L_1$  to  $L_4$ , and pivot locations (Appendix A). Because the precise location of the potentiometer pivots was difficult to determine, the location of the roller, as determined by the Data Acquisition System, is not necessarily correct. A small offset was therefore allowed for in the location of each pair of potentiometer pivots. To determine the offsets, a series of cyclic control sweeps was carried out with a Black Hawk (Section 4.3). Table 3 shows potentiometer pivot locations before and after corrections were applied. Corrected values were used in the algorithm.

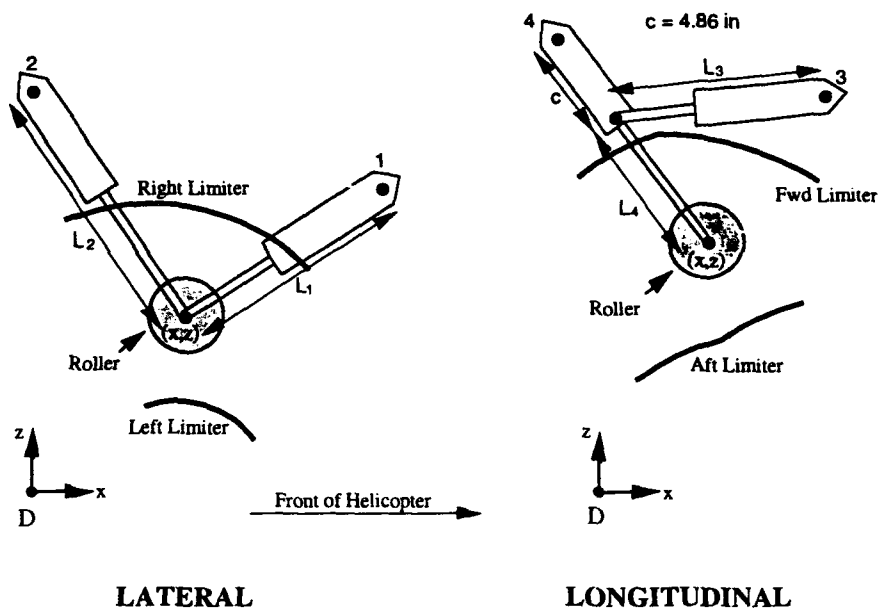


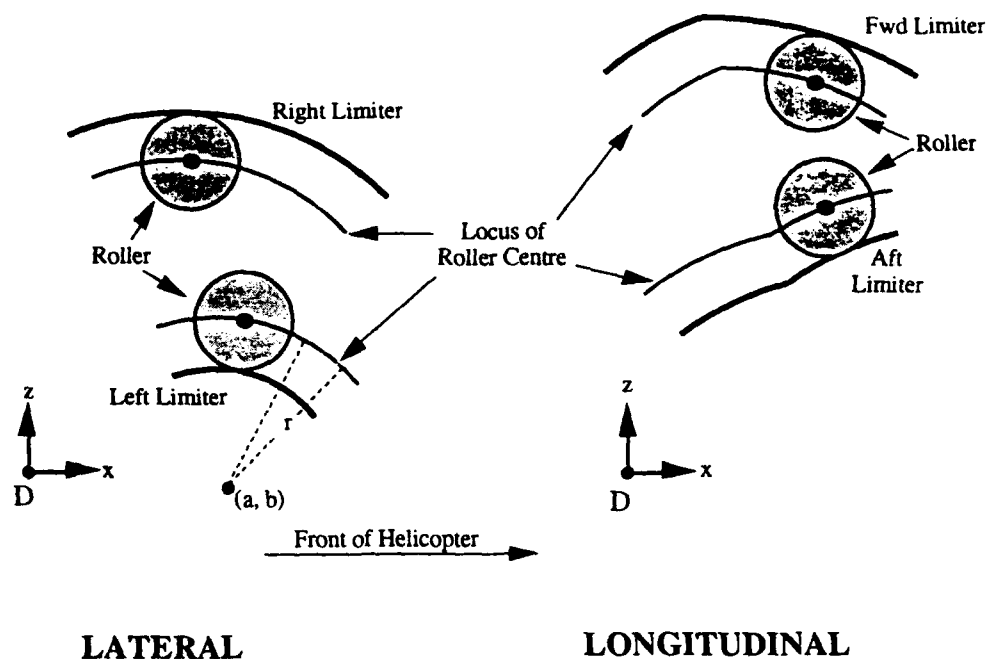
Fig. 5 Location of Potentiometers Used to Determine Roller Location

TABLE 3  
Location of Potentiometer Pivots Relative to D (STA=292, WL=274)

Potentiometer	Location	x		z	
		Uncorrected	Corrected	Uncorrected	Corrected
1	Fwd Lateral	8.16	8.26	4.89	4.77
2	Aft Lateral	0.30	0.40	8.37	8.25
3	Fwd Longitudinal	6.39	6.82	8.94	8.89
4	Aft Longitudinal	-2.03	-1.60	11.19	11.14

#### 4.2 Limiter Geometry

The limiters are shown in Fig. 6. For the lateral case, each limiter is the arc of a circle. For the longitudinal case, each limiter comprises two adjoining circular arcs. The equations representing the limiters (i.e. radius and location of centre) were determined from engineering drawings. Using a roller radius of 0.72 inch, the equations representing the path of the roller centre as it traverses along a limiter (Fig. 6) can then be determined.



**Fig. 6 Location of Mixer Unit Limiters and Locus of Roller Centres**

While the radius of each circle comprising each limiter was accurately known from engineering drawings, the location of the centre of each limiter circle had to be estimated. A small offset was therefore allowed for in the location of the centre of each circular arc comprising the limiters. To determine the offsets, a series of tests was carried out on a Black Hawk. The pilot controls were moved so that, where possible, the roller moved along each limiter in turn. Several readings for roller location were taken for each circular arc and a least squares process was then used to determine the centre (a,b) of the best fit circle with the radius  $r$  fixed at the value determined from engineering drawings (Table 4). Corrected values for circle centre locations show discrepancies of up to 0.23 inch (Table 4).

**TABLE 4**  
**Circle Parameters for Roller Centre as Roller runs along Limiters**  
**(Dimensions in Inches)**

Circle Parameter	Left Lateral Arc (Lower Limiter)		Right Lateral Arc (Upper Limiter)		Aft Longitudinal Arc (Lower Limiter)				Fwd Longitudinal Arc (Upper Limiter)			
					Rear		Front		Rear		Front	
	Predicted	Derived	Predicted	Derived	Predicted	Derived	Predicted	Derived	Predicted	Derived	Predicted	Derived
a	2.65	2.65	2.22	2.22*	3.30	3.44	4.36	4.59	2.681	2.844	1.237	1.393
b	-0.47	-0.43	1.14	1.17*	-0.97	-0.98	-0.79	-0.76	2.329	2.306	0.973	0.987
r	2.43		2.968		3.57		3.80		3.28		4.48	

\* Because the roller touches the right limiter at only a very limited region (see Fig. 3 - Lateral Nomogram), the right lateral limiter correction could only be estimated. The correction obtained for the left lateral limiter was used in the estimation since corrections for the longitudinal limiters (with the exception of the aft front) show some consistency.

### 4.3 Effect of Control Inputs on Roller Motion

The location of each roller in the mixer unit, together with labels for key dimensions, are shown in Fig. 7. Pivots C and E are able to move relative to the fixed pivot D in response to control inputs. The longitudinal and lateral rollers are similar except that the dimensions of some of the control arms are different.

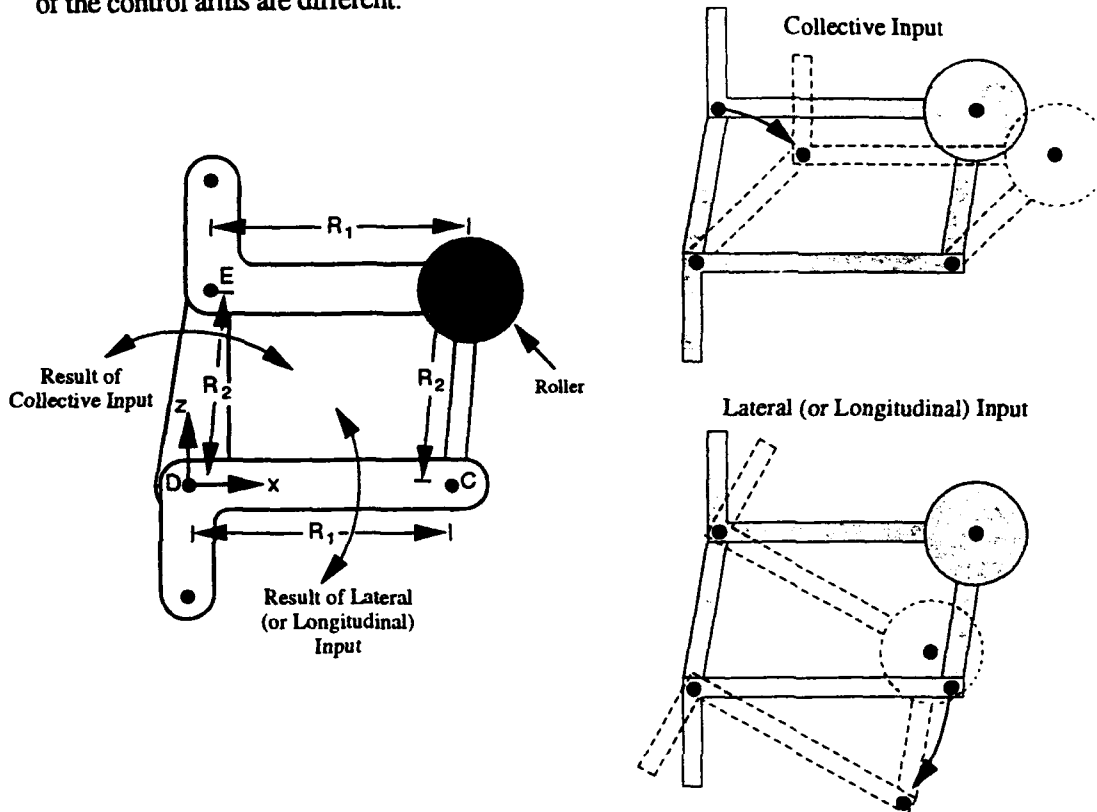
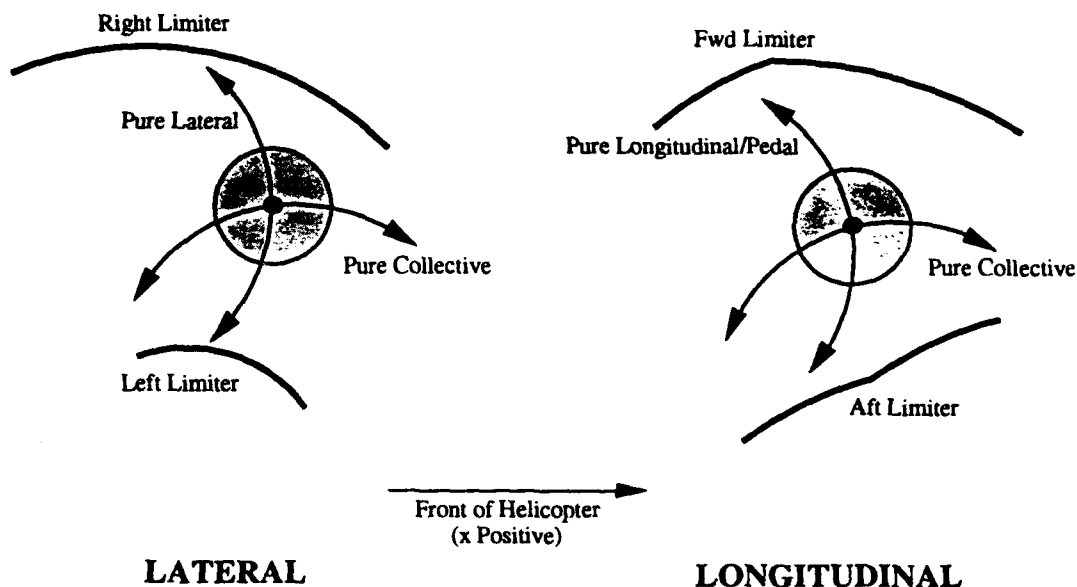


Fig. 7 Schematic Showing Effect of Various Control Inputs on Roller Location

Referring to Fig. 7, pure lateral (or longitudinal) input causes C to rotate about D while E is held fixed. The result is that the roller is able to move in a circular arc of radius  $R_1$  about E. Pure collective input causes E to rotate about D with C held fixed. The result is that the roller moves in a circular arc of radius  $R_2$  about C, with the location of C depending on the lateral (or longitudinal) input. In addition, pedal inputs cause modification to the longitudinal input for the longitudinal roller. The roller movement is summarised in Fig. 8. During flight, a combination of control inputs is applied, resulting in complex motion of each roller. Values for  $R_1$  and  $R_2$ , determined from engineering drawings, are given in Table 5.

TABLE 5  
Radius Arm Lengths in Mixer Unit

	Radius Arm Length (in)	
	$R_1$	$R_2$
Lateral	3.13	2.48
Longitudinal	3.13	3.24



**Fig. 8 Schematic Showing Roller Movement Dependence on Control Inputs**

In summary, for variation of a single control input (collective or cyclic), the roller moves in a circular arc about a moveable centre. For pure cyclic input, the circle centre is E, which itself lies on a circular arc radius  $R_2$  and centre D. For pure collective input, the circle centre is C, which lies on a circular arc radius  $R_1$  and centre D.

As mentioned in Section 4.1, the location of the potentiometer pivots, required in the calculation of roller location, was not accurately known. To determine a correction to each pivot pair, a series of cyclic sweeps was carried out at three collective settings. Several measurements for roller location were taken for each cyclic sweep (see lateral example given in Fig. 9) and a least squares process was used to calculate the centre of each best fit circle of known radius  $R_1$  (Table 5). The centres correspond to point E (Fig. 7). Ideally, these should lie on a circle centre D and radius  $R_2$ . However, because of measurement inaccuracies, the circle centre will be at a location, D' say, that is offset from D. The least squares program was then used again, with the coordinates of the various values of E (i.e.  $E_1, E_2, E_3$ ) and with known radius  $R_2$  (Table 5), to determine the offset of D' from D (Table 6). The pivot locations were then corrected in the algorithm using these offsets to ensure that the measurements were accurately referenced to D.

**TABLE 6**  
**Offsets Due to Measurement Inaccuracies in Potentiometer Pivot Locations**

	Offset between D' and D Prior to Potentiometer Pivot Location Correction	
	x Offset (in)	z Offset (in)
Lateral	-0.10	0.12
Longitudinal	-0.43	0.05

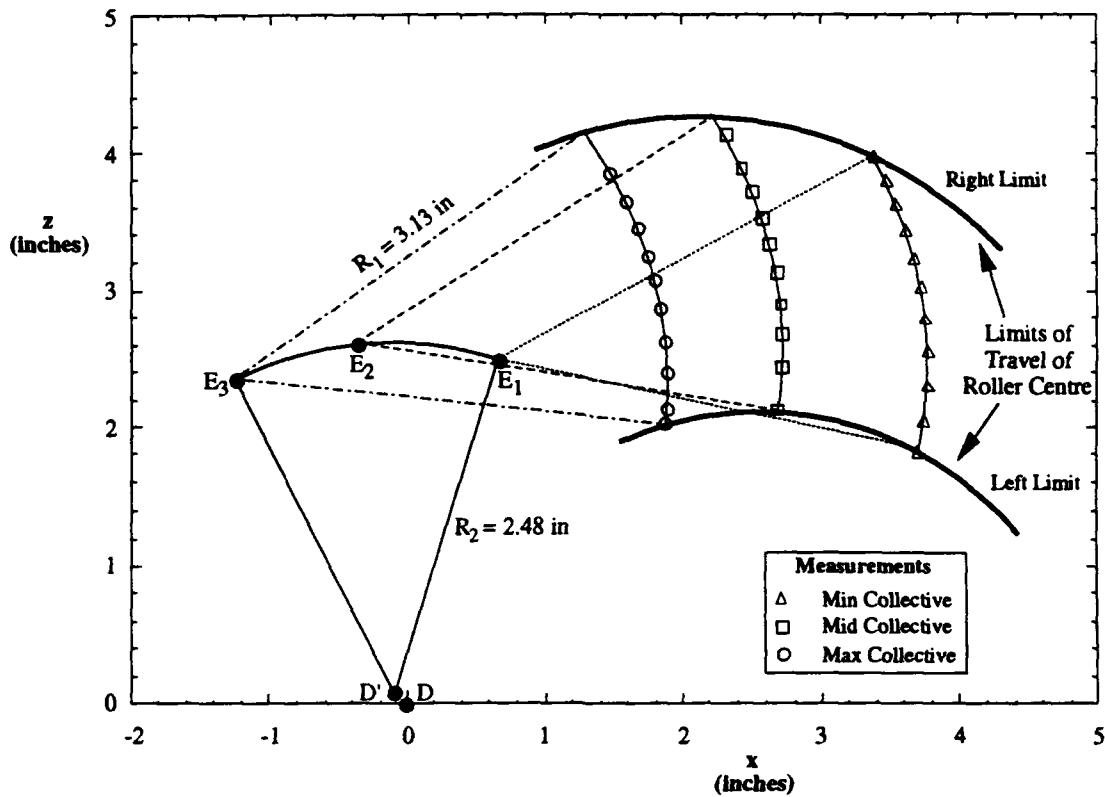


**Fig. 9 Path Followed by Lateral Roller for Pure Lateral Sweep at Various Fixed Collective Settings**

#### 4.4 Fraction of Possible Primary Control Movement

Given the location  $(x_k, z_k)$  of the roller, as determined from the potentiometer lengths and pivot locations (Appendix A), it is possible to deduce the fraction of allowable control movement. In the following analysis, refer to Fig. 10, which is a schematic showing lateral roller location. The longitudinal case is similar except that 0 and 100% limits are reversed.

It has been determined (Section 4.3) that pure cyclic variation at fixed collective results in a circular path for each roller with radius  $R_1$  and centre E. Defining the coordinates of E as (A,B), the equation for the circular arc through  $(x_k, z_k)$  is given by

$$R_1^2 = (x_k - A)^2 + (z_k - B)^2 \quad (1)$$

with A and B being unknown. The path followed by point E for pure collective variation is circular with radius  $R_2$  and centre at reference point D, resulting in the expression

$$R_2^2 = A^2 + B^2 \quad (2)$$

Equations (1) and (2) are solved simultaneously to determine quantities A and B (Appendix B). The equation for the circular arc representing pure cyclic variation through  $(x_k, z_k)$  is now known, and the intersection of this arc with the lower limiter,  $(x', z')$ , and upper limiter,  $(x'', z'')$ , is easily determined (Appendix B).



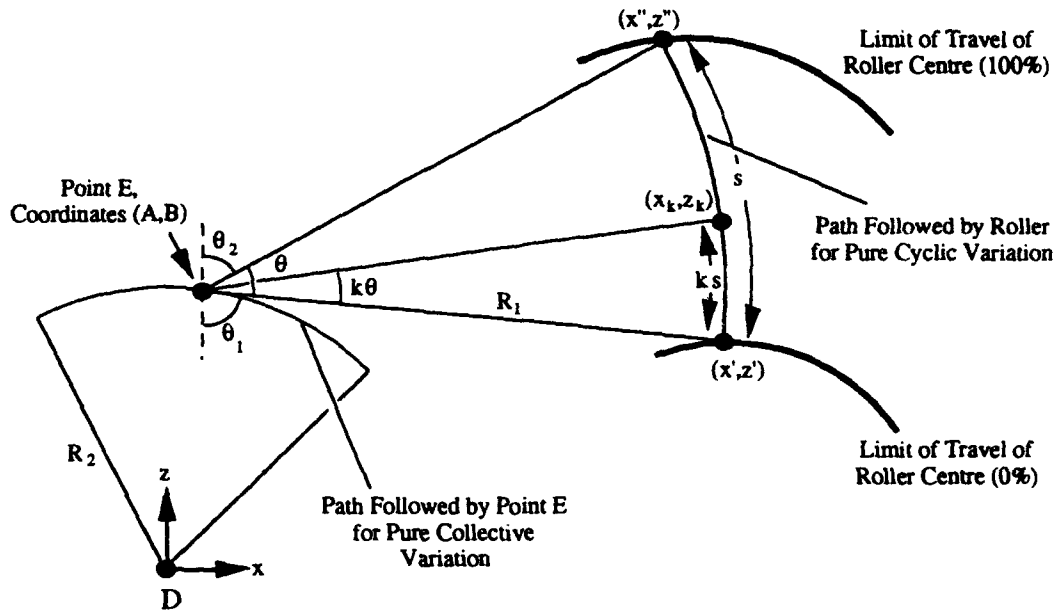


**Fig. 10 Determination of Percentage of Allowable Lateral Control Movement**

The fraction of allowable control movement represented by point  $(x_k, z_k)$  is determined by calculating the fraction of arc length  $s$  between the two limiters, or equivalently the fraction of angle  $\theta$ . If  $k$  is the fraction between 0 and 1, then from Fig. 10

$$x_k = A + R_1 \sin(\theta_1 + k\theta) \quad (3)$$

$$z_k = B - R_1 \cos(\theta_1 + k\theta) \quad (4)$$

where

$$\theta_1 = \arcsin\left(\frac{x' - A}{R_1}\right) \quad (B > z') \quad (5a)$$

$$= \pi - \arcsin\left(\frac{x' - A}{R_1}\right) \quad (B < z') \quad (5b)$$

$$\theta_2 = \arcsin\left(\frac{x'' - A}{R_1}\right) \quad (6)$$

$$\theta = \pi - (\theta_1 + \theta_2) \quad (7)$$

Rearranging, the fraction of control movement is given by

$$k = \frac{\arcsin\left(\frac{x_k - A}{R_1}\right) - \theta_1}{\theta} \quad (8)$$

where  $k = 0$  (0% of possible primary control movement) represents the lower limiter and  $k = 1$  (100% of possible primary control movement) represents the upper limiter (Fig. 10). For the longitudinal roller, where the lower limiter represents 100% of possible primary control movement and the upper limiter represents 0% of possible primary control movement,  $(1-k)$  should be substituted for  $k$ .

The above analysis was used in two ways. The first was to determine percentage of control movement given roller location. The resultant algorithm, which was not able to be run at real time during the FOCFT due to computer power limitations, was used for analysis after the trial for converting time traces of roller location to time traces of primary control position (Section 6). The second application of the analysis was to construct an array of points representing 0, 10, 15, 85, 90, and 100% of allowable control range. This array was used by a fast algorithm which was able to be run in real time during the FOCFT. The aim of this algorithm was first to determine which region of allowable control movement the primary controls were in, and then to turn cockpit lights on or off when appropriate. This algorithm is discussed in more detail in Section 5. The arrays generated are shown in Fig. 11 (showing coordinates of the roller centre) and Fig. 12 (after converting back to potentiometer lengths as required by the algorithm). In addition, a 350 point check array was generated for each roller to assist in the checking of the light-switching algorithm (Section 5). Details on the array generation are given in Appendix C.

It is anticipated that for future trials, a more powerful data acquisition system will allow the full algorithm to be run in real time. The algorithm could be used to operate either cockpit lights or gauges. The gauges would display a continuous reading of control authority remaining relative to primary stops.

## **5. ALGORITHM TO OPERATE COCKPIT LIGHTS**

### **5.1 General Description**

The algorithm that operates the cockpit lights, which runs in real time, is designed to operate with the VADAR system. This system can acquire 32 channels of analog data, six channels of synchro data, and eight bits of both digital input and output at various acquisition rates. The algorithm takes input from six analog channels and provides five channels of digital output to drive cockpit mounted lights. A check is made of channel sampling rates to determine whether all of the data acquisition input channels required for the algorithm to operate are being sampled. These include the four potentiometer lengths ( $L_1$ ,  $L_2$ ,  $L_3$ ,  $L_4$ ) representing primary lateral and longitudinal control positions, as well as the primary collective and tail rotor control positions. If one or more of these channels is not sampled, then there is insufficient information available and the algorithm is prevented from running. After each sample is acquired, the measured value is converted to engineering units (inches for the potentiometer measurements, and percent control authority for primary tail rotor and collective position). The algorithm then determines whether any primary limits have been reached, and sets the appropriate cockpit lights.

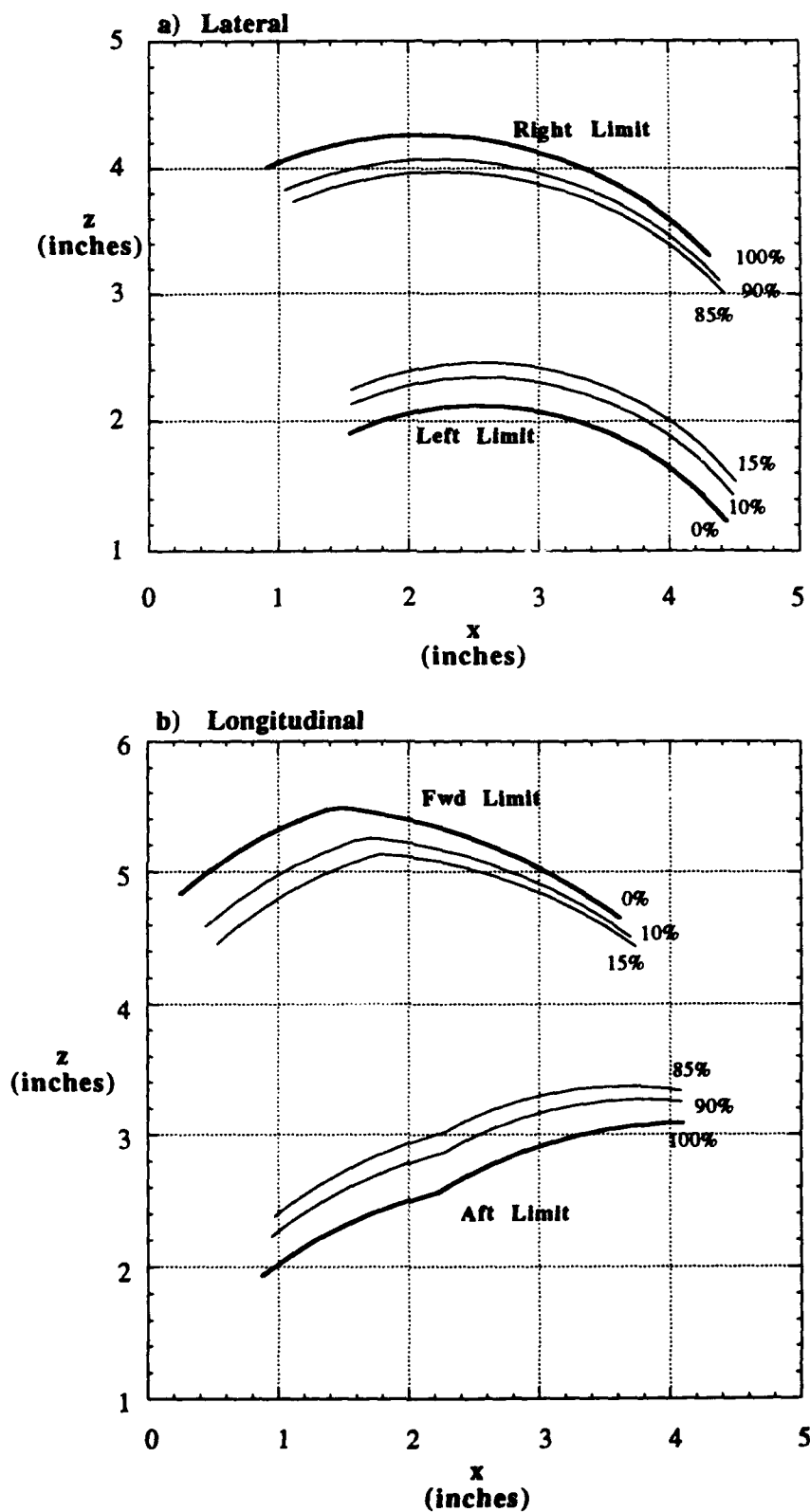


**Fig. 11 Allowable Primary Control Movement - Roller Displacement**

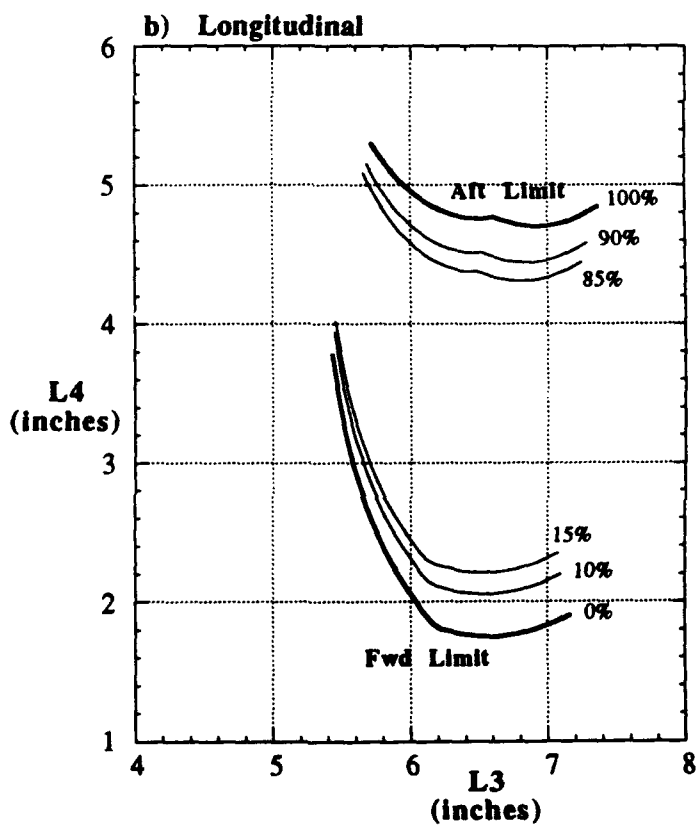
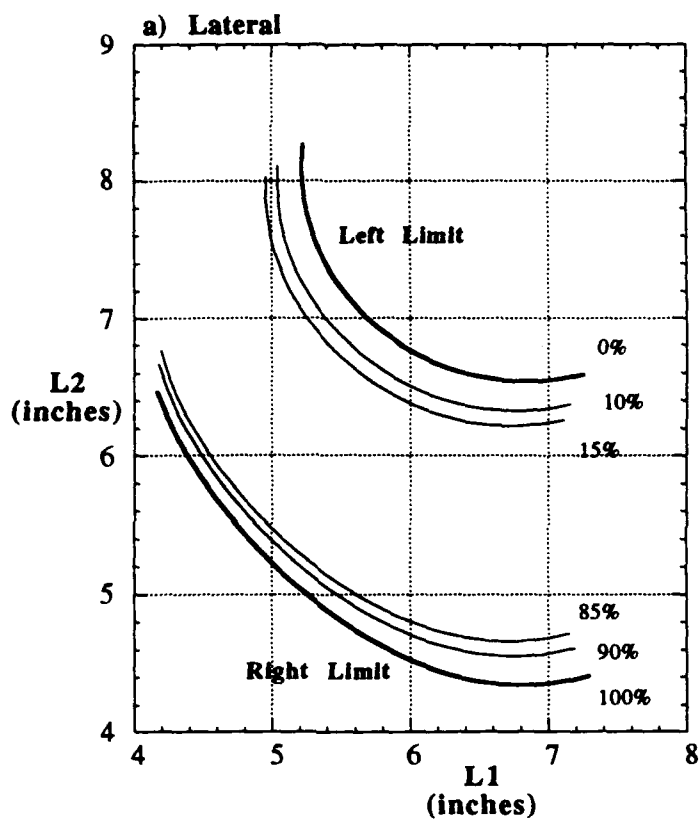


**Fig. 12 Allowable Primary Control Movement - Potentiometer Lengths**

## 5.2 Algorithm Details

Two separate algorithms were implemented, one for the primary collective and tail rotor positions, and another for the primary lateral and longitudinal control positions.

Each algorithm determines the region that the control inputs are operating within for a particular data sampling period. The regions determined are 0-10%, 10-15%, 15-85%, 85-90%, and 90-100%. For all of the control inputs, the acceptable operating region is 15-85% control authority. The regions 10-15% and 85-90% result in an amber cockpit warning light being energised for that channel. If any control input reaches the regions 0-10% or 90-100%, then a single red cockpit light is energised. The only exception to this is for the primary collective control, where the 0-15% region does not operate lights. This is to avoid unnecessary warnings prior to takeoff, when the collective stick will be in a lowered position.

### 5.2.1 Primary Collective and Tail Rotor Position Algorithm

The primary collective and tail rotor position algorithm compares the measured control inputs, calibrated in units of percentage control authority, with the allowable limits to determine the required operating region. The allowable limits are easily determined since, in each case, the control movement is linear and control stops are fixed rather than variable.

### 5.2.2 Primary Lateral and Longitudinal Control Limits Algorithm

The algorithm to determine primary lateral and longitudinal control position is more complicated than the collective and tail rotor position algorithm due to the end stops being variable rather than fixed. When the data acquisition package is first started, the data arrays which describe the length of the linear potentiometers at each of the "limit positions" for both lateral and longitudinal control movement (Section 4.4) are read into the algorithm. In these arrays,  $L_2$  and  $L_4$  determine limit positions at 0, 10, 15, 85, 90, and 100% for given  $L_1$  and  $L_3$  (Fig. 12). Given measured potentiometer lengths  $L_1$  and  $L_3$  as read in by the data acquisition system, which may not agree exactly with array values, interpolation between array points is required in order that  $L_2$  and  $L_4$  can be determined at each limit position for the measured  $L_1$  and  $L_3$ . The measured values of  $L_2$  and  $L_4$  are then compared to the interpolated limit values of  $L_2$  and  $L_4$  to determine which region the roller is currently in. To illustrate the interpolation method used, an example is given in Fig. 13. This figure shows an enlarged portion of Fig. 12a, showing only part of the 85, 90, and 100% lateral array limits. In Fig. 13, two consecutive points in the lateral array for the 90% limit are  $(L_1, L_2) = (4.54, 5.93)$  and  $(4.46, 6.05)$ . A measurement value of  $L_1$  equal to 4.50 inches would, by interpolation, have an estimated 90% limit at  $L_2 = 5.99$  inches. By similar means, the 100% limit for this measured  $L_1$  is deduced as  $L_2 = 5.82$  inches. If the corresponding measurement of  $L_2$ , as recorded by the data acquisition system, is 5.97 inches, by comparison with the interpolated values of  $L_2$  this measurement point is seen to lie in the 90-100% region.

The interpolation procedure is made complicated near the extremities of each data set because it is not always possible to determine an interpolated value of  $L_2$  (or  $L_4$ ) for all of the limit percent values (e.g. in Fig. 12, for a potentiometer length  $L_1$  equal to 4.5 inches, there is no 0, 10, or 15% value of  $L_2$ ). Three distinct cases were identified, and a method for dealing with each was developed. The three cases are identified by three regions, which are shown in Fig. 14 for the lateral primary controls (corresponding to Fig. 12a). The method developed applies also to the longitudinal primary control (by replacing  $L_1$  and  $L_2$  by  $L_3$  and  $L_4$  respectively, and reversing percentage limits, e.g. 0 and 100%).

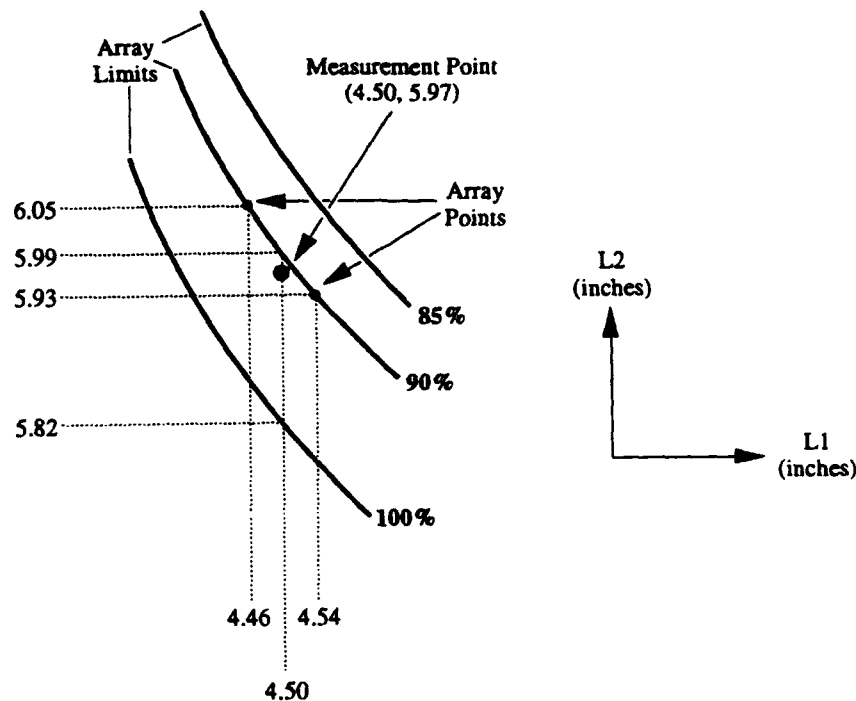


**Fig. 13 Interpolation Example Using Lateral Array**

**Case 1**

This is the most frequently occurring case. Interpolated percent values for  $L_2$  exist on either side of the measured value of  $L_2$ . It is relatively straightforward to first compare the measured value of  $L_2$  with each of the interpolated percent values and then determine the region the roller must lie in. For example, the measured values for  $L_1$  and  $L_2$  at Point 1 in Region 1 put the roller in the region 10-15%.

**Case 2**

This case occurs with moderate frequency. A number of interpolation points for  $L_2$  are not successful, and there are none above the measured value of  $L_2$ . Given that roller movement is limited by a geometrical relationship between the linkages (Fig. 7), in addition to the two physical limiters, and that the arrays have data points which extend to the extremities, then the roller must lie between the percentage limit directly beneath the measured value and the next limit up. For example, at Point 2 in Region 2, the measured values for  $L_1$  and  $L_2$  place the roller in the region 15-85%. The same procedure applies when there are no successful interpolation points for  $L_2$  below its measured value. Here, the roller must lie between the percentage limit immediately above the measured value and the next limit down.

**Case 3**

The least likely case is when there are valid interpolated values for  $L_2$  both above and below the measured value, including one directly above but not directly below (or one directly below but not directly above). In this case it is possible to deduce that the roller is in a region defined by the valid data points, but it cannot be narrowed down to one region alone. For example, successful interpolation is only possible at Point 3 in Region 3 for 0, 10, 15, and 100%. Given the absence of any other interpolated percent values, it is not possible to say anything beyond that the roller lies between 15 and 100%. The precise percentage range could be determined if the geometrical limitations were input as additional array elements, but this was not done because of time limitations when developing the algorithm for the Black Hawk FOCFT. Also, additional software may have taken the run time for the algorithm over the limit required for 20 Hz sampling

(Section 5.2.4). Using the data check arrays (Appendix C), it was found that the algorithm only resulted in points falling in Region 3 for four out of 350 check points. Case 3 is therefore treated as an error condition and, rather than giving possible erroneous light indications, all lights are left off. The algorithm would be expected to encounter a normal operating point (i.e. Case 1 or 2), which would trigger the lights, shortly before or shortly after reaching this error condition, and so the pilot would still be aware of crossing any limit.

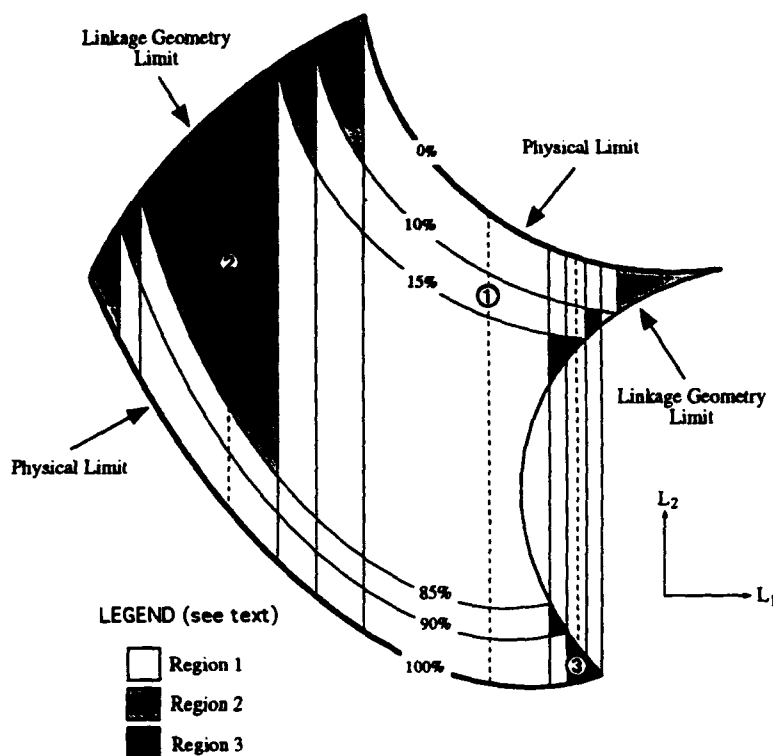


Fig. 14 Location Regions for Primary Lateral Roller

### 5.2.3 Light Switching

As described in Section 5.2, the algorithm switches (a) four amber lights to indicate that the respective channel is within 15% of its control authority limit and (b) one red light to indicate that one of the channels is within 10% of its control authority limit. If a 10% limit is encountered, then the algorithm energises the single red light as well as the amber light corresponding to the channel going into that condition. This ensures that, if between successive samples the roller moves rapidly from a 15-85% normal region to that of 10% control authority input remaining (i.e. 0-10% or 90-100% region), then the pilot is able to determine which channel has reached this limit. However, this is considered unlikely due to the relatively slow movement of the roller in comparison to the data acquisition rate of 20 Hz. In Fig. 15, the operation of the lights for primary tail rotor position is illustrated for a non-flying test where the pedals were moved while the helicopter was sitting on the ground. Both amber and red lights functioned as required.

Additional hardware, developed by AMAFTU, allows each of the lights to be either "latched" or free-running. In the latched mode, if a control input ever becomes limited (less than 15% control authority remaining), even for a brief period, the appropriate light remains on after being activated so that it is not likely to be missed by the pilot. The pilot is able to unlatch the light at any time. In the free-running mode, the light status is constantly updated by the algorithm at a rate of 20 Hz. In either case, data are stored in the free-running mode for post-trial analysis. The

hardware energises the appropriate light when a logic value of one is set by the algorithm on the digital output port.

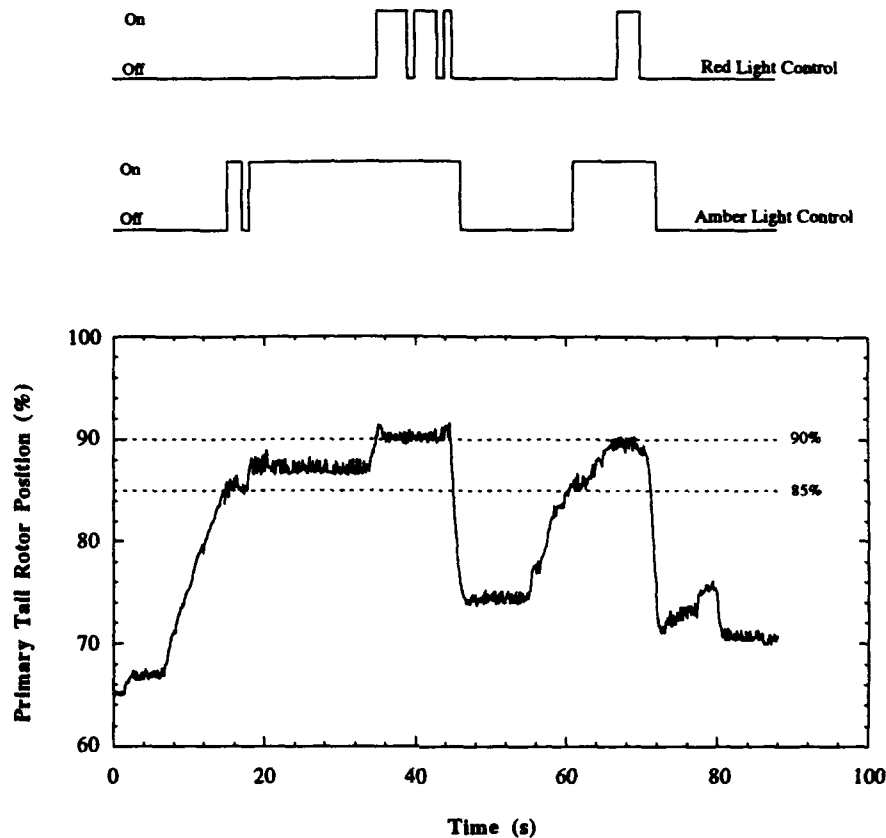


**Fig. 15 Operation of Primary Tail Rotor Lights for a Non-Flying Test Case**

#### **5.2.4 Algorithm Execution Time**

As the system is required to operate in real time, the execution time of the algorithm will, to a large extent, determine the maximum data acquisition rate of the system. With the currently used computer, a Compaq Portable with an 80286 processor and 80287 coprocessor, execution time was measured at 23 ms. This equates to a maximum sampling rate of 20 Hz after taking into account the execution time of the data acquisition program. Utilising a faster and more powerful 80386/80387 processor, the execution time was measured at 12 ms, which would allow a sampling rate of 40 Hz.

Considerable modification of the data acquisition software was required to allow the system to be "interrupt driven" so that any processor idle time could be utilised by the algorithm.



## **6. PRELIMINARY RESULTS FROM FIRST OF CLASS FLIGHT TRIALS**

The FOCFT involved 162 recorded take-offs and 171 recorded landings at different gross weights and centre of gravity (cg) positions. Take-offs and landings were performed during the day and night, in different sea states, and with various wind-over-deck speeds and directions. In addition, a series of specified control input manoeuvres (step inputs in collective and cyclic at various forward speeds, with SAS on and off) was performed at the request of ARL to create data for control system analysis at a later date. Three such manoeuvres are illustrated below. Results shown are preliminary only and involve no analysis. The purpose is to show that the control system instrumentation and algorithm functioned during-flight and to illustrate the effect on control margins of mechanical control mixing and AFCS inputs (in particular the SAS). The primary and secondary control positions, as a percentage of full control travel, are shown as a function of time during each manoeuvre, together with resultant angular rates, linear accelerations, and pitch and roll attitude (yaw attitude was not measured) for the helicopter. To produce the results below, raw data from the VADAR were converted to the required engineering units using calibration factors obtained prior to the trial. Primary lateral and longitudinal control positions were then determined by applying the calculations given in Section 4.4.

### **6.1 Effect of Mechanical Control Mixing**

Fig. 16 shows results for a collective step input with SAS off. Though the pilot does not apply any significant input to other controls, the mechanical mixing results in a significant step input to the primary tail rotor (yaw) control and a small step input to the lateral and longitudinal primary controls. The large amount of collective-yaw mixing is of particular interest since, without control mixing, a collective step down of 15% with other controls held fixed (as in Fig. 16) would result in significant yaw to the left. Yet as a result of collective-yaw mixing, yaw is virtually eliminated (the yaw rate is only 3 deg/s).

### **6.2 Effect of AFCS Inputs**

The effect of a longitudinal step input is shown in Fig. 17 with SAS off and in Fig. 18 with SAS on. With SAS off, it should be noted that primary control movements follow secondary movements quite closely, though there is a translation of a few percent due to differing control limits. In particular, there is a step in the primary longitudinal control (output) that closely follows the step input in the secondary longitudinal control (pilot input). However, with SAS on, the primary longitudinal control is returned to its original value in spite of the pilot input (secondary control) remaining at its deviated value. This comparison clearly illustrates the effect of the SAS in providing additional control inputs between the pilot inputs and the primary outputs. In terms of available longitudinal control movement, secondary longitudinal controls are about 60% from the forward limiter in both cases after the step input, whereas the primary longitudinal control is about 55% from the forward limiter for SAS off, and about 45% for SAS on. The minimum of primary and secondary control remaining, in this case 55% for SAS off and 45% for SAS on, determines the resultant control remaining relative to the forward limiters. The change in control authority as a result of using the SAS is clearly demonstrated for the case presented.

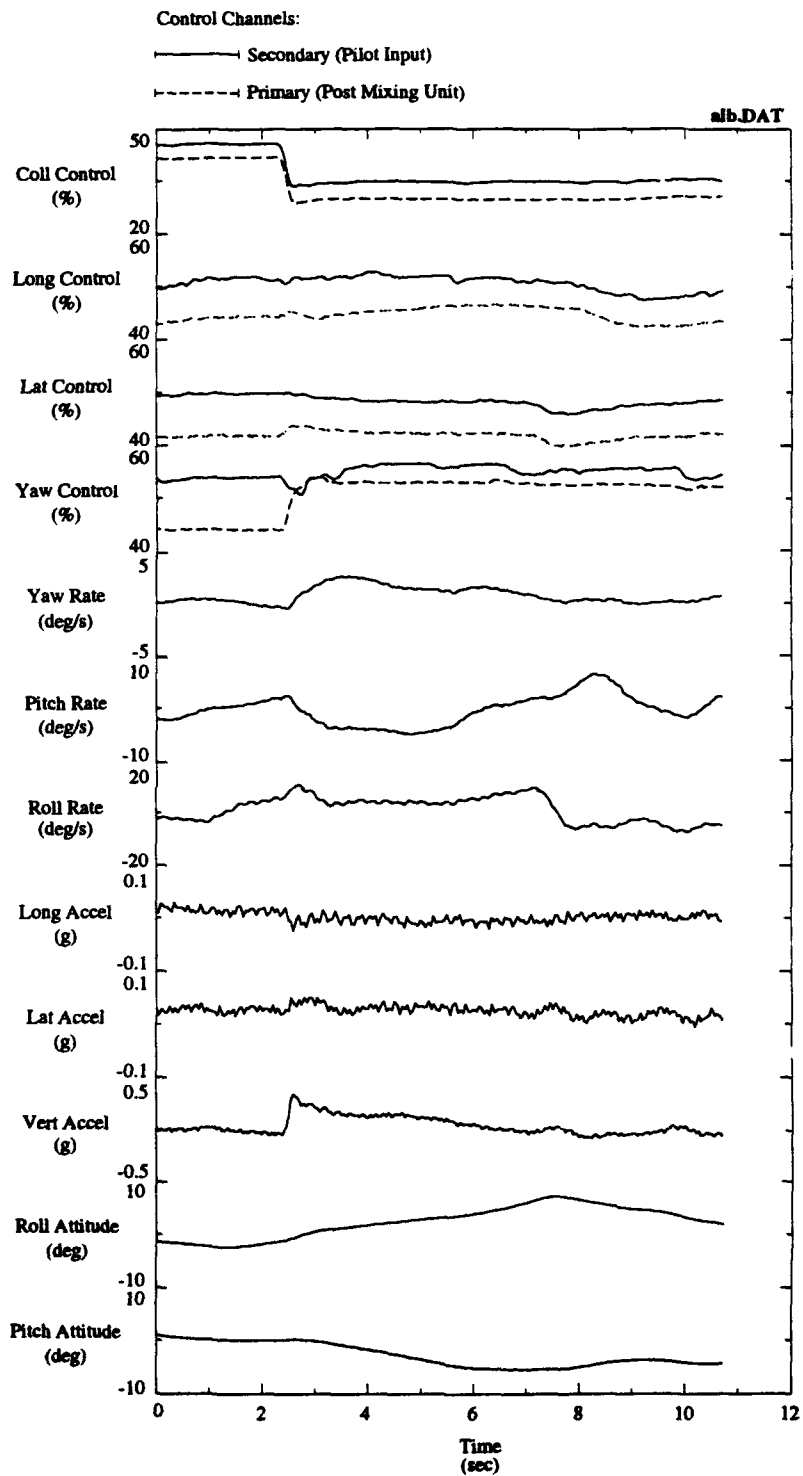
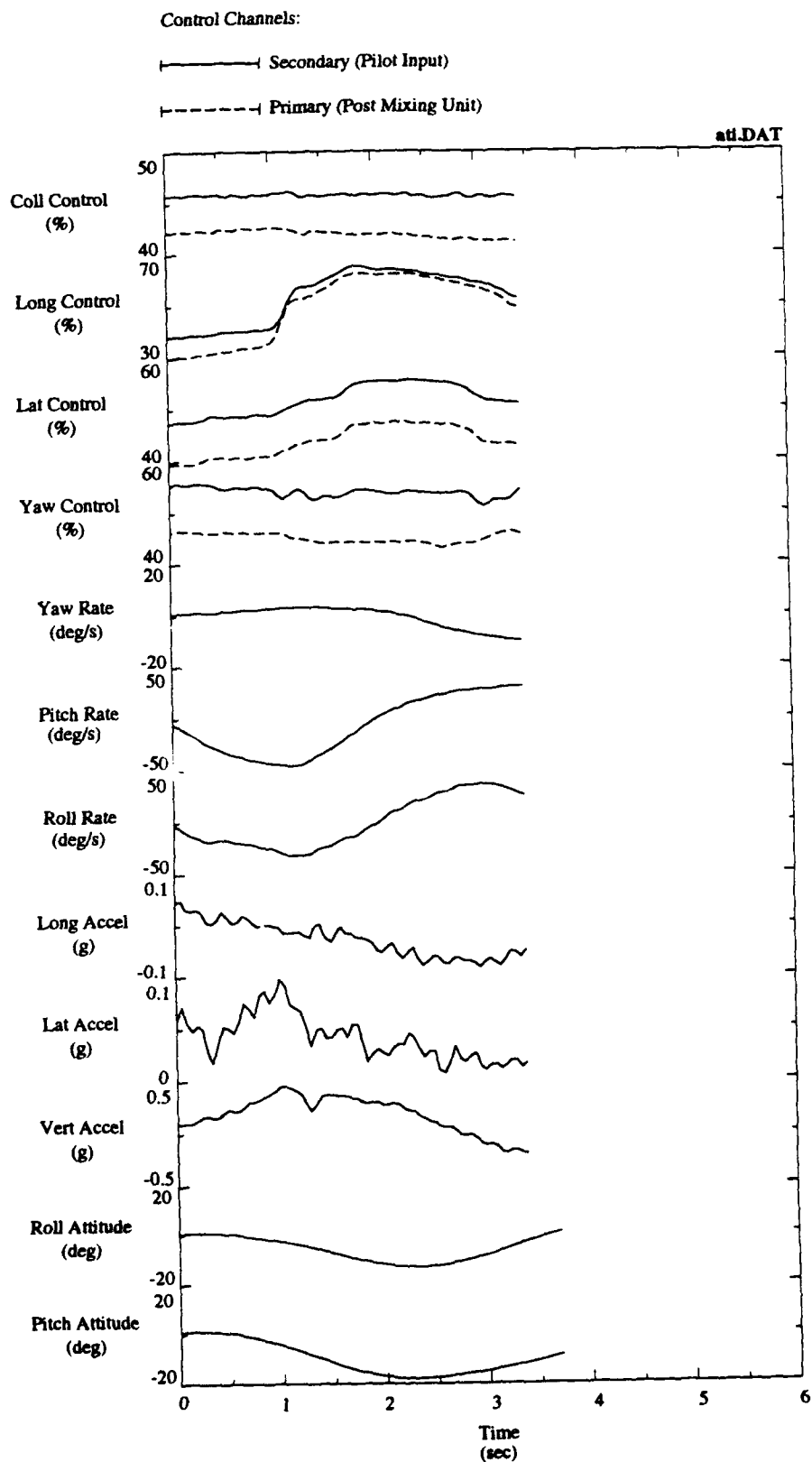
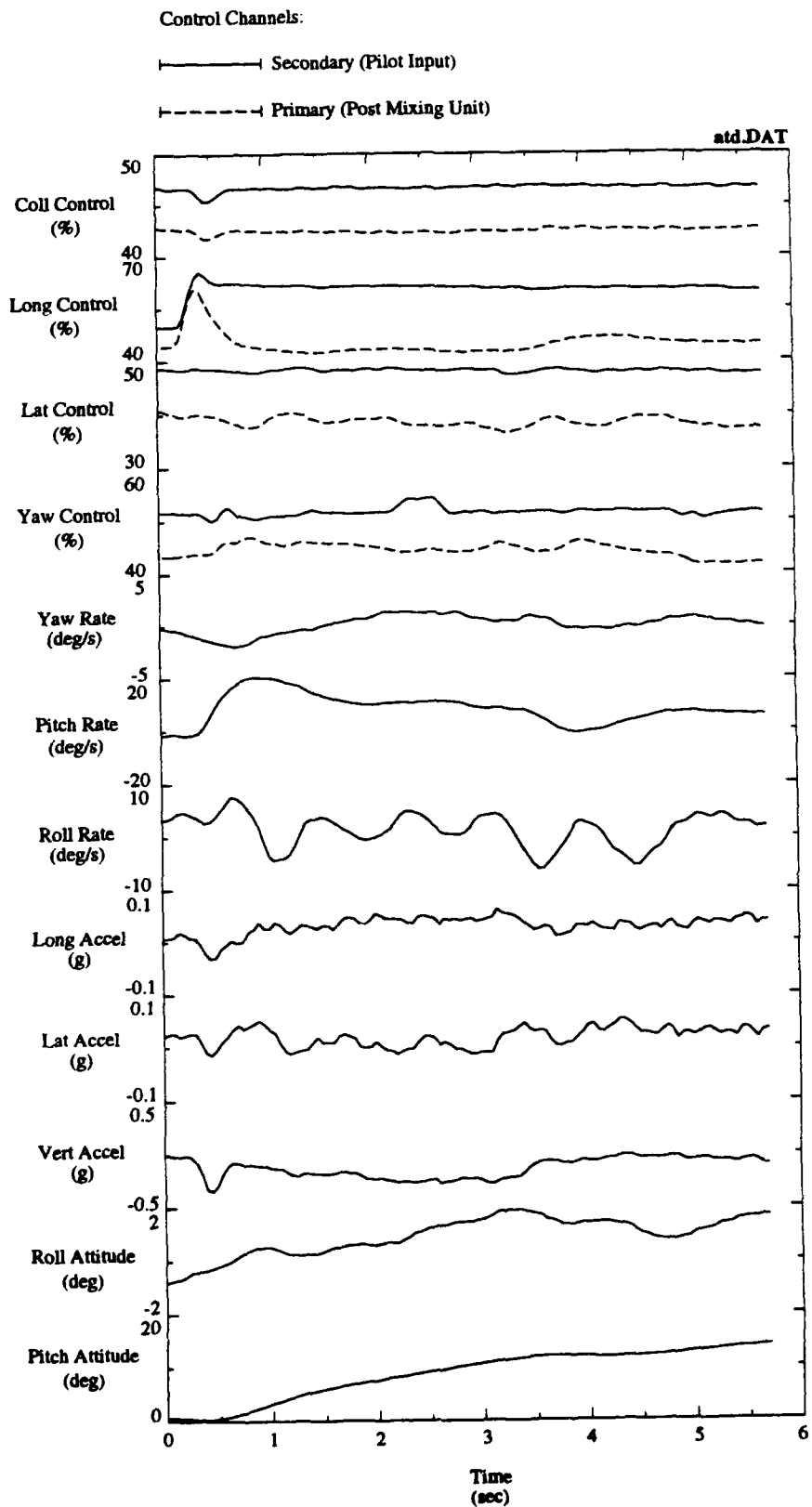


Fig. 16 Results for Collective Down Step Input at 60 Knots (SAS Off)



**Fig. 17 Results for Aft Longitudinal Step Input at 60 Knots (SAS Off)**



**Fig. 18 Results for Aft Longitudinal Step Input at 60 Knots (SAS On)**

## 7. CONCLUDING REMARKS

A procedure has been developed to instrument and record control positions relative to primary limits on Black Hawk and Seahawk helicopters while in flight. Results are fed to an algorithm, which runs in real time. The algorithm operates individual amber lights if a primary control approaches to within 15% of a limit, and a single red light if any primary control approaches to within 10% of a limit. An additional algorithm has also been developed which can determine actual control authority remaining, rather than whether controls have exceeded various limits. This algorithm does not run in real time with the current data acquisition system, but improvements in computer hardware should make this possible for future trials. The algorithm can be readily used for post-trial analysis.

To the authors' knowledge, the recording of cyclic control position relative to primary limits has not been done before for Black Hawk or Seahawk helicopters. There were a number of problems encountered. In particular, determining the amount of available control travel remaining was difficult due to the non-linear motion of these controls in the vicinity of limiters. In addition, the instrumentation of control position required much ingenuity because of the lack of available space to mount transducers.

The procedure was used successfully in a recent FOCFT and illustrated the effect of mechanical control mixing and the AFCS. Together with the instrumentation of secondary controls (used on an earlier trial with a Seahawk), it is now possible to monitor the amount of control authority remaining and determine when it is minimal. This will enable important information to be obtained when developing helicopter/ship operational limits.

## ACKNOWLEDGMENTS

The authors wish to thank staff at AMAFTU for assistance given during the lead up to the FOCFT and for supplying trial data afterwards, as well as Owen Holland of ARL for his part in the generation of the light-switching algorithm.

## REFERENCES

1. RAN AMAFTU Trials Report on HMAS Tobruk/Black Hawk S-70A-9 (*to be published*).
2. Howlett, J.J., UH-60A Black Hawk Engineering Simulation Program: Vol II - Background Report, NASA CR-166310, December 1981.
3. Pilots Flight Manual, RAN Role-Adaptable Weapon System: S-70B-2 Aircraft, NAP 7210.024-1-1, September 1987.
4. Flight Manual-Black Hawk S-70A-9, AAP 7210.015-1, August 1989.
5. Holland, O.F., Harvey, J.F., and Sutton, C.W., "A Versatile Airborne Data Acquisition and Replay (VADAR) system," *ARL Flight Mechanics Document (to be published)*.
6. Sikorsky Aircraft Drawings for Black Hawk, Prefix 70400, Drawing Numbers 02242, 02244, 02287, 02288, 22300.

## APPENDIX A

### DETERMINATION OF ROLLER LOCATION GIVEN POTENTIOMETER LENGTHS

#### A.1 Lateral

From Fig. A1,

$$L = \sqrt{(x_1 - x_2)^2 + (z_2 - z_1)^2} \quad (A1)$$

$$\psi = \arccos \left( \frac{L^2 + L_1^2 - L_2^2}{2 L L_1} \right) \quad (\text{cosine rule}) \quad (A2)$$

$$\gamma = \arctan \left( \frac{z_2 - z_1}{x_1 - x_2} \right) \quad (A3)$$

$$\theta = \psi - \gamma \quad (A4)$$

The location of the centre of the lateral roller is given by

$$x = x_1 - L_1 \cos \theta \quad (A5)$$

$$z = z_1 - L_1 \sin \theta \quad (A6)$$

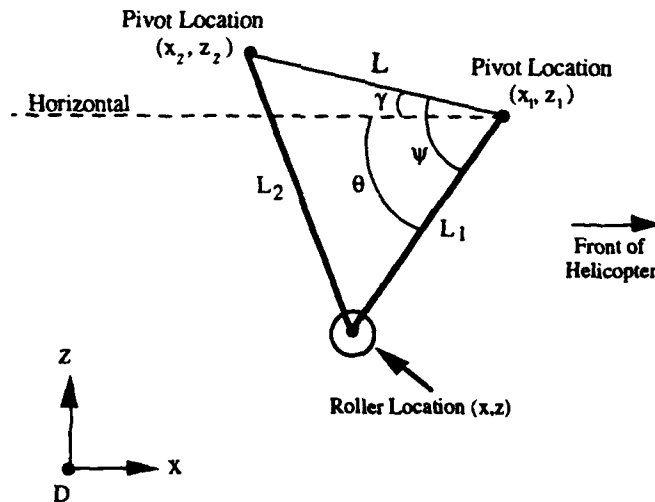


**Fig. A1 Relationship between Lateral Potentiometer Lengths and Location of Centre of Roller**

## A.2 Longitudinal

From Fig. A2,

$$L = \sqrt{(x_3 - x_4)^2 + (z_4 - z_3)^2} \quad (A7)$$

$$\psi = \arccos \left( \frac{L^2 + c^2 - L_3^2}{2 L c} \right) \quad (\text{cosine rule}) \quad (A8)$$

$$\gamma = \arctan \left( \frac{z_4 - z_3}{x_3 - x_4} \right) \quad (A9)$$

$$\theta = \psi + \gamma \quad (A10)$$

The location of the centre of the longitudinal roller is given by

$$x = x_4 + (c + L_4) \cos \theta \quad (A11)$$

$$z = z_4 - (c + L_4) \sin \theta \quad (A12)$$

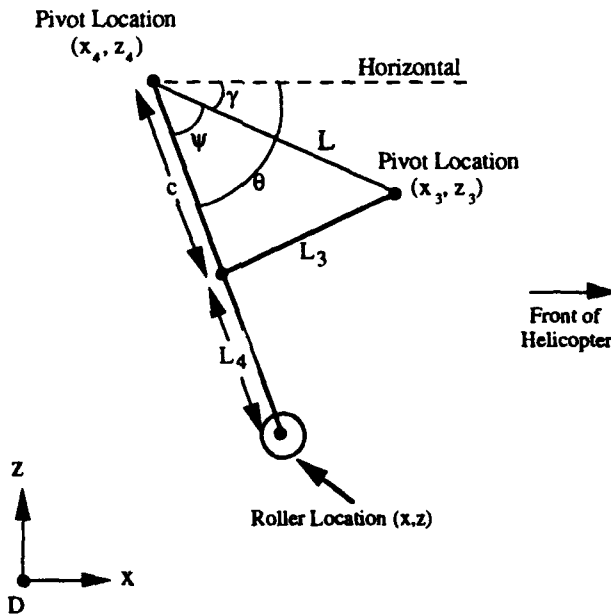


**Fig. A2 Relationship between Longitudinal Potentiometer Lengths and Location of Centre of Roller**

## APPENDIX B

### DETERMINATION OF THE INTERSECTION OF TWO CIRCLES

Consider two circles with different radii  $r$  and  $R$  and different locations of centre  $(a,b)$  and  $(A,B)$  represented by the following equations:

$$(x - a)^2 + (z - b)^2 = r^2 \quad (B1)$$

$$(x - A)^2 + (z - B)^2 = R^2 \quad (B2)$$

Let their intersection be point  $(x_i, z_i)$ . Coordinate  $z_i$  can be determined from (B1) given  $x_i$ , and inserted in (B2) to give

$$\left(\sqrt{r^2 - (x_i - a)^2} + (b - B)\right)^2 + (x_i - A)^2 = R^2 \quad (B3)$$

Expanding the left side results in

$$2(b - B)\sqrt{r^2 - (x_i - a)^2} + (b - B)^2 + (r^2 - (x_i - a)^2) + (x_i - A)^2 = R^2 \quad (B4)$$

Rearranging and squaring both sides gives

$$r^2 - (x_i - a)^2 = \left[ \frac{R^2 - (b - B)^2 - (r^2 - (x_i - a)^2) - (x_i - A)^2}{2(b - B)} \right]^2 \quad (B5)$$

or

$$\begin{aligned} r^2 - (x_i^2 - 2ax_i + a^2) &= \left[ \frac{R^2 - r^2 - (b - B)^2 + (x_i^2 - 2ax_i + a^2) - (x_i^2 - 2Ax_i + A^2)}{2(b - B)} \right]^2 \\ &= \left[ F + \frac{x_i(A - a)}{(b - B)} \right]^2 \end{aligned} \quad (B6)$$

where

$$F = \frac{(R^2 - r^2) - (b - B)^2 + (a^2 - A^2)}{2(b - B)} \quad (B7)$$

Rewriting (B6) as a quadratic in  $x_i$  results in

$$Cx_i^2 + Dx_i + E = 0 \quad (B8)$$

where

$$C = 1 + \left( \frac{A - a}{b - B} \right)^2 \quad (B9)$$

$$D = 2 \left( \frac{F(A - a)}{(b - B)} - a \right) \quad (B10)$$

$$E = F^2 + a^2 - r^2 \quad (B11)$$

Coordinate  $x_i$  can be solved for in the usual manner and  $z_i$  then determined using either Equation (B1) or (B2).



The specific example referred to by Equations (1) and (2) of Section 4.4 results in

$$C = 1 + \left(\frac{-x_k}{z_k}\right)^2 \quad (\text{B12})$$

$$D = 2 \left( F \left( \frac{-x_k}{z_k} \right) - x_k \right) \quad (\text{B13})$$

$$E = F^2 + x_k^2 - R_1^2 \quad (\text{B14})$$

with

$$F = \frac{(R_2^2 - R_1^2) - z_k^2 + x_k^2}{2z_k} \quad (\text{B15})$$

## APPENDIX C

### CONSTRUCTION OF ARRAY FOR LIGHT SWITCHING ALGORITHM

Referring to Fig. 10, select a value of A and calculate B from Equation (2). A single circular arc has now been defined by centre (A,B) and radius  $R_1$ . Using Appendix B, it is possible to determine where this arc meets the lower limiter ( $x',z'$ ) and upper limiter ( $x'',z''$ ). For a given collective (equivalent to the selected value of A), the range of allowable primary control movement is now known and the percentage of allowable control movement can be determined. If k is the fraction of allowable roller movement between 0 and 1, then the location of the kth point on the arc of pure cyclic variation, ( $x_k, z_k$ ), is determined by Equations (3) and (4), where  $\theta$ ,  $\theta_1$ , and  $\theta_2$  are given in Equations (5) to (7).

A single point ( $x_k, z_k$ ) has now been generated which corresponds to a single value of A (equivalent to a given collective setting). By now incrementing A to cover the full x range of each limiter, an array representing the kth fraction of allowable roller movement is generated. An increment size of 0.1 inch was selected for A resulting in 31 and 32 points being required for the lateral and longitudinal limiter arrays respectively. Arrays are generated for 0, 10, 15, 85, 90, and 100% (Fig. 11). The coordinates ( $x_k, z_k$ ) are converted back to potentiometer lengths, ( $L_1, L_2$ ) for lateral and ( $L_3, L_4$ ) for longitudinal, to create the array required by the light switching algorithm (Fig. 12). The same procedure was also used for intermediate values of k to generate a check array in order to test the light switching algorithm. The check array was generated for two fixed percentage values per region, where the five regions are defined as 0-10%, 10-15%, 15-85%, 85-90%, and 90-100%. For example, for region 0-10%, check points were generated corresponding to 1 and 9% of possible primary control movement. A total of 35 points per percentage value was generated, resulting in a total of 350 points in the check array.

## **DISTRIBUTION**

### **AUSTRALIA**

#### **DEPARTMENT OF DEFENCE**

##### **Defence Central**

Chief Defence Scientist  
AS, Science Corporate Management  
FAS, Science Policy  
Director, Departmental Publications  
Counsellor, Defence Science, London (Doc Data Sheet only)  
Counsellor, Defence Science, Washington (Doc Data Sheet only)  
Office of Naval Attache, Washington  
Scientific Adviser, Defence Central  
OIC TRS, Defence Central Library  
Document Exchange Centre, DSTIC (8 copies)  
Defence Intelligence Organisation  
Librarian H Block, Victoria Barracks, Melbourne (Doc Data Sheet only)

} shared copy

##### **Aeronautical Research Laboratory**

Director  
Library  
Chief - Flight Mechanics and Propulsion Division  
Chief - Aircraft Systems Division  
Chief - Aircraft Structures and Materials Division  
Branch File - Flight Mechanics  
Authors: J. Blackwell  
S. Dutton  
R. Toffoletto  
J. F. Harvey  
R.A. Feik (ANL TTCP HTP-6)  
N.E. Gilbert (4 copies)  
C.A. Martin  
N. Pollock  
C.W. Sutton (2 copies)

##### **Materials Research Laboratory**

Director/Library

##### **Defence Science & Technology Organisation - Salisbury**

Library

##### **Navy Office**

Navy Scientific Adviser  
Aircraft Maintenance and Flight Trials Unit (2 copies)  
Director Armament Engineering - Navy  
Director of Aircraft Engineering - Navy  
Director of Naval Air Warfare  
Superintendent, Aircraft Logistics - Naval Support Command  
Helicopter Project Director - Navy

**Army Office**

Scientific Adviser - Army  
Engineering Development Establishment, Library  
US Army Research, Development and Standardisation Group

**Air Force Office**

Air Force Scientific Adviser (Doc Data Sheet only)  
Aircraft Research and Development Unit  
Scientific Flight Group  
Library  
Engineering Branch Library  
OIC ATF (2 copies)

**HQ ADF**

Director General Force Development (Air)

**CANADA****Defence Research Establishment, Atlantic**

J.L. Colwell

**National Research Council, Ottawa**

M. Sinclair (Canadian NL TTCP HTP-6)

**Bombardier Inc., Canadair, Montreal**

B.I.K. Ferrier

**UNITED KINGDOM****Defence Research Agency, Bedford**

G.D. Padfield

B. Tomlinson

**Defence Research Agency, Farnborough**

A.F. Jones (UKNL TTCP HTP-6)

**UNITED STATES****US Army Aeroflightdynamics Directorate, Ames Research Center**

W.G. Bousman (USNL TTCP HTP-6)

M. Eshow

D.L. Key

**NASA, Ames Research Center**

M.G. Ballin

J.L. Cross

S. Jacklin

R. Kufeld

W.J. Snyder

J. Totah

W.G. Warmbrodt

**Naval Air Warfare Center, Aircraft Division, Warminster**  
J.W. Clark, Jr (TTCP HTP-6)  
J. Funk

**Naval Air Warfare Center, Aircraft Division, Patuxent River**  
D. Carico  
L. Trick  
G.M. VanderVliet

**Johnson Aeronautics**  
W. Johnson

**Advanced Rotorcraft Tecnology**  
R. Du Val

**SPARES (6 copies)**

**TOTAL (80 copies)**

**DOCUMENT CONTROL DATA**PAGE CLASSIFICATION  
UNCLASSIFIED

PRIVACY MARKING

1a. AR NUMBER AR-007-083	1b. ESTABLISHMENT NUMBER ARL-FLIGHT- MECH-R-191	2. DOCUMENT DATE OCTOBER 1992	3. TASK NUMBER NAV 92/019
4. TITLE VARIABLE CONTROL SYSTEM LIMITS ON BLACK HAWK AND SEAHAWK HELICOPTERS		5. SECURITY CLASSIFICATION (PLACE APPROPRIATE CLASSIFICATION IN BOX(S) IE. SECRET (S), CONF. (C) RESTRICTED (R), LIMITED (L) UNCLASSIFIED (U)).  <div style="display: flex; justify-content: space-around;"> <div style="border: 1px solid black; padding: 2px; text-align: center;">U</div> <div style="border: 1px solid black; padding: 2px; text-align: center;">U</div> <div style="border: 1px solid black; padding: 2px; text-align: center;">U</div> </div> DOCUMENT      TITLE      ABSTRACT	6. NO. PAGES  32  7. NO. REFS.  6
8. AUTHOR(S) J. BLACKWELL, S. DUTTON R. TOFFOLETTO, J.F. HARVEY		9. DOWNGRADING/DELIMITING INSTRUCTIONS  Not applicable.	
10. CORPORATE AUTHOR AND ADDRESS  AERONAUTICAL RESEARCH LABORATORY  506 LORIMER STREET FISHERMENS BEND VIC 3207		11. OFFICE/POSITION RESPONSIBLE FOR: SPONSOR <u>NAVY</u> SECURITY <u>-</u> DOWNGRADING <u>-</u> APPROVAL <u>CFPD</u>	
12. SECONDARY DISTRIBUTION (OF THIS DOCUMENT)  Approved for public release.  OVERSEAS ENQUIRIES OUTSIDE STATED LIMITATIONS SHOULD BE REFERRED THROUGH DSTIC, ADMINISTRATIVE SERVICES BRANCH, DEPARTMENT OF DEFENCE, ANZAC PARK WEST OFFICES, ACT 2601			
13a. THIS DOCUMENT MAY BE ANNOUNCED IN CATALOGUES AND AWARENESS SERVICES AVAILABLE TO . . .  No limitations.			
13b. CITATION FOR OTHER PURPOSES (IE. CASUAL ANNOUNCEMENT) MAY BE		<input checked="" type="checkbox"/> UNRESTRICTED OR <input type="checkbox"/> AS FOR 13a.	
14. DESCRIPTORS UH-60A helicopters S-70B helicopters Control equipment Flight control systems Flight management systems			15. DISCAT SUBJECT CATEGORIES 0104 010301
16. ABSTRACT <i>Black Hawk and Seahawk helicopters have various fixed physical control limits situated throughout the control system. The range of each pilot control is variable and depends on which limit is reached first. This is a function of the pilot control inputs applied, together with any additional control inputs provided by the automatic flight control system. A procedure has been developed to monitor controls in the vicinity of each limit, and determine if any part of the control system approaches to within a prescribed amount of a limit. Warning lights in the cockpit inform the pilot if a limit is being approached. The procedure was used effectively during a First of Class Flight Trial involving a Black Hawk.</i>			

PAGE CLASSIFICATION  
**UNCLASSIFIED**

PRIVACY MARKING

THIS PAGE IS TO BE USED TO RECORD INFORMATION WHICH IS REQUIRED BY THE ESTABLISHMENT FOR ITS OWN USE BUT WHICH WILL NOT BE ADDED TO THE DISIS DATA UNLESS SPECIFICALLY REQUESTED.

16. ABSTRACT (CONT).

17. IMPRINT

**AERONAUTICAL RESEARCH LABORATORY, MELBOURNE**

18. DOCUMENT SERIES AND NUMBER

Flight Mechanics Report 191

19. COST CODE

51-526J

20. TYPE OF REPORT AND PERIOD COVERED

21. COMPUTER PROGRAMS USED

22. ESTABLISHMENT FILE REF.(S)

23. ADDITIONAL INFORMATION (AS REQUIRED)